The sum of the above values (355) represents the whole-house permeability. The stack permeability constant was estimated to be equal to 385 CF/min per inch H_2O and therefore —

$$X \text{ for house and stack} = 740 \text{ CF/min per inch } H_2O$$

This value agrees rather well with the earlier estimated value (712) evolved at by using Equation 21 and the measured pressures.

The specific assumptions and data used in these calculations are —

Pressure Differences

$$\Delta P_x = -0.0030 \text{ inch } H_2O \text{ with stack open}$$

$$\Delta P_x = -0.0035 \text{ inch } H_2O \text{ with stack closed}$$

Crack Permeability

Flow through cracks, at a pressure difference of 0.3 inch H_2O is —

	CF/min-ft of cracks
Windows (weatherstripped)	0.5
Doors (with storms)	0.7
Framing and sill plates	0.25

The agreement, achieved with reasonable assumptions, suggests that windows, doors, framing and sill plate cracks account for most of the permeable component inventory.

Static Probe Placement

Considerable "noise" was observed in the indoor-outdoor static pressure measurements, during periods when wind speeds were appreciable, even when the reference probe was located 60 feet from the "neutral" side of the house. We do not know to what extent this is a reflection of the actual pressure fluctuations in the house or of kinetic effects of vertical components of the wind on the reference outdoor probes.

Relocation of the reference probe in the attic did appreciably damp out the fluctuations. However, during periods when the wind direction was fluctuating rapidly at a relatively low wind speed (≈5 mph), the indoor-attic static pressure difference was observed to fluctuate. For example, it decreased (i.e., became more negative) when the wind was easterly (normal to the opening to both the living space and to the attic) and became less negative

when the wind was southerly (normal to the south wall, which has no openings to either the living space or the attic).

This finding is in direct contrast with the wind effects observed when the indoor-outdoor static pressure differences were measured with the reference probe located outdoors. In the latter case, the easterly winds impinging on the broadside openings of the house increased the pressure in the house. We can explain the behavior if we assume that the winds impinging on the openings to both the attic and living space result in a greater increase in the pressure in the attic ($K_x/K_i = 1$; $\frac{\Delta Px}{\Delta Pw} = 0.5$) than in the living space ($K_x/K_i = 1.84$; $\frac{\Delta Px}{\Delta Pw} = 0.22$). It is apparent, however, that the attic cannot be used as the reference probe for indoor-outdoor static pressure difference measurements.

Locating the reference probe about 40 feet away into a relatively dense woods, gave the "best" results. At least some of the noise was damped out, and the wind effects on ΔP made sense. In particular, a 3-mph wind impinging on the south wall, which has no openings to the living space, had no effect including "noise" on the indoor-outdoor static pressure differences or on the "noise" when the reference probe was located in the woods. Thus, the noise usually observed with a wind of that magnitude was not affecting the house or the reference probe.

Wind Effect on Static Pressure Difference

We were surprised at the effect that very low wind speeds had on the indoor-outdoor static pressure differences. For example, wind speeds as low as 2 to 3 mph resulted in significant static pressure fluctuations (of the order of 0.002 inches of H_2O), when the indoor-outdoor temperature difference approached zero and the blower was off. Admittedly, there is little net effect of these very low wind speeds on the average indoor-outdoor pressure difference. However, the resultant dynamic fluctuations can in fact account for the base-line infiltration rate of 0.07 air changes per hour observed under the no-driving-force conditions.

These effects would lead us to believe that each static pressure excursion from positive to negative observed on the windward side of the house results in a small amount of infiltration-exfiltration of air, together with some mixing because of kinetic forces on the outside and on the inside of the wall.

Simultaneously, the same excursion also causes a small exfiltration-infiltration on the other side of the house, with mixing inside and outside being enhanced by the kinetic motion of the air. The result may be a pumping action.

2. Two-Story Dwellings

In addition to the single-story, heavily instrumented, unoccupied home (except for the test personnel), we acquired two additional 2-story homes (usually free of the owner-occupants during measurements) to carry out specific tests relating to effects of buoyancy and shielding. Of these, one was a 6-room, two story, all brick home (30 years of age) with a gross living area of 2200 square feet, and with shielding on the 2 sides due to adjacent buildings.

In the former 2-story home, full communication is provided between the furnace room and the rest of the house. In the latter, only minimal interaction is available since the furnace is located in the attached garage (underneath the second floor bedrooms). Both of these installations contribute to house infiltration differently and represent the two most significant variations in home construction controlling the effect of furnace operation on house infiltration.

One objective of the test program scheduled for these homes is to determine the effect that the second floor barrier may have on air infiltration rates, when these are primarily driven by buoyancy forces (i.e., high indoor-outdoor temperature differences at low wind speed). Another objective is to obtain the effect of shielding when the infiltration motive force is mainly wind velocity (at essentially zero indoor-outdoor temperature difference). Preliminary infiltration data from these two homes are summarized in Table 4 and 5. Additional data are currently being generated to provide full delineation of these effects.

B. Extensive Field Testing

A significant amount of data is available from the 23 test homes, obtained during 1977 as part of the A.G.A. project HC-4-33,[21] and most, if not all, of these data are of relevent value to this phase of the program. The main thrust of this phase of extensive testing in the 23 homes has been the development of data relating indoor-outdoor temperature differences to the respective driving forces affecting infiltration as they vary from one type of home to another. Therefore, the test program during 1978 concentrated primarily in measurements of pressure differences that provided

Table 4. BASE-LINE DATA FROM 2-STORY TEST HOME WITH INDOOR FURNACE

Run No.	Furnace Mode			Avg. Wind Conditions		Avg. Temperatures		Infiltration Rates
	Blower	Furnace	Stack	Speed, mph	Direction	In	Out	air changes/hr
1a	On	Off	Closed	12	South	68°F	60°F	0.33
2a	On	Off	Closed	12	South	71°F	57°F	0.38
1b	Off	Off	Closed	12	South	68°F	60°F	0.18
1c	On	Off	Open	12	South	68°F	60°F	0.39
2b	On	Off	Open	12	South	71°F	57°F	0.40
1d	Off	On	Open	12	South	68°F	60°F	0.29
1e	On	On	Open	12	South	68°F	60°F	0.60
2c	On	On	Open	12	South	71°F	57°F	0.74
A	On	Off	Closed	12	Southwest	68°F	70°F	0.48
A	On	Off	Open	12	Southwest	68°F	70°F	0.48
A	On	On	Open	12	Southwest	68°F	70°F	0.60
C	On	Off	Closed	15	South	70°F	63°F	0.43
C	On	On	Open	15	South	70°F	63°F	0.55
D	On	Off	Closed	3	Southwest	68°F	37°F	0.69
D	On	On	Open	3	Southwest	68°F	37°F	0.85
E	On	Off	Closed	10	Southwest	68°F	6°f	0.89
E	On	On	Open	10	Southwest	68°F	6°F	1.31

Table 5. BASE-LINE DATA FROM THE 2-STORY TEST HOME WITH FURNACE IN THE GARAGE

Run No.	Furnace Mode			Avg. Wind Conditions		Avg. Temperatures		Infiltration Rates,
	Blower	Furnace	Stack	Speed, mph	Direction	In	Out	air changes/hr
1a	On	Off	Closed	8	Southwest	72	54	0.80
2a	On	Off	Closed	11	Southwest	70	53	0.91
3a	On	Off	Closed	13	Southwest	68	50	0.39
1b	Off	Off	Closed	8	Southwest	72	54	0.44
1c	On	Off	Closed	8	Southwest	72	54	0.68
2b	On	Off	Open	11	Southwest	70	53	0.74
3b	On	Off	Open	13	Southwest	68	50	0.43
1e	On	On	Open	8	Southwest	72	54	0.68
2c	On	On	Open	11	Southwest	70	53	0.74
3c	On	On	Open	13	Southwest	68	50	0.44

the basic understanding in the formulation of the IGT model of air infiltration.

1. Background

As discussed earlier (section entitled, "Intensive" Field Testing), the indoor-outdoor pressure differential can be directly measured by placing a probe, connected to the other leg of the sensor, indoors. However, in the field homes, the measurements were found to be highly sensitive to wind gusts and vehicular traffic. Initially measured pressure differences exhibited large variations ranging from -0.02 inches of water to over + 0.03 inches of water column over short time periods.

The tests were carried out in 8 of the 23 field test homes and, in order to reduce these effects on the differential pressure measurements, the outdoor leg of the sensor was placed in the attic of the house (Figure 24). A typical trace obtained by the attic or indirect method is shown in Figure 25. Although there are still significant variations in the measured pressure differential, the fluctuations were considerably dampened. However, the data may not be very accurate (as discussed in the earlier section) and are presented here only to illustrate the relative effects of important variables on pressure levels.

The dampening effect was sufficient to allow us to obtain a time-averaged pressure differential, by inspection of the trace of Figure 25. The ΔP_x, or indoor-outdoor pressure difference at a particular height above ground level, is calculated from the measured pressure difference (ΔP_m) through Equation 22, which corrects for the pressure differential represented by the column of air between the reference and the attic levels.

$$\Delta P_x(h) = \Delta P_m - 7.66L(1/T_o - 1/T_i) \qquad (22)$$

where

ΔP_m = measured pressure differential, in. H_2O
L = height of attic probe above sensor, ft
T_o = outdoor temperature, °R
T_i = indoor temperature, °R.

The indirect or attic method was used to determine the pressure distributions in 8 test homes. In most cases it was difficult to compare the attic

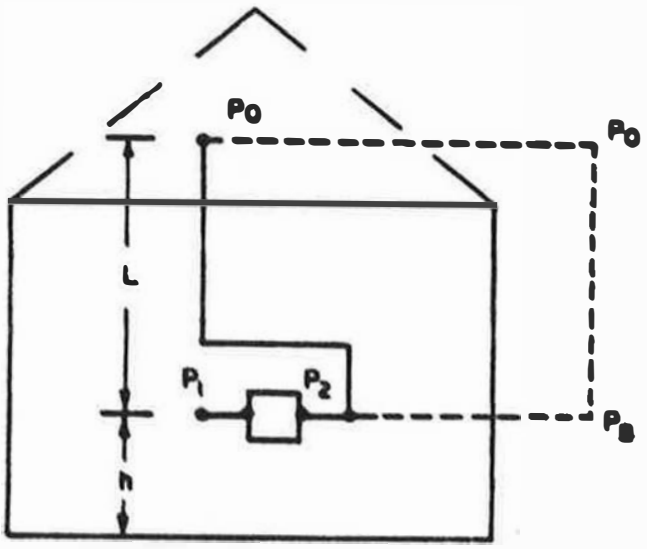

$$\Delta P_x(h) = (P_1 - P_B) = \left[(P_1 - P_2) - 7.66\,L(1/T_o - 1/T_i)\right] \text{ in. } H_2O$$

A7805M433

Figure 24. INDIRECT MEASUREMENT OF ΔP_x WITH PROBE PLACED IN THE ATTIC

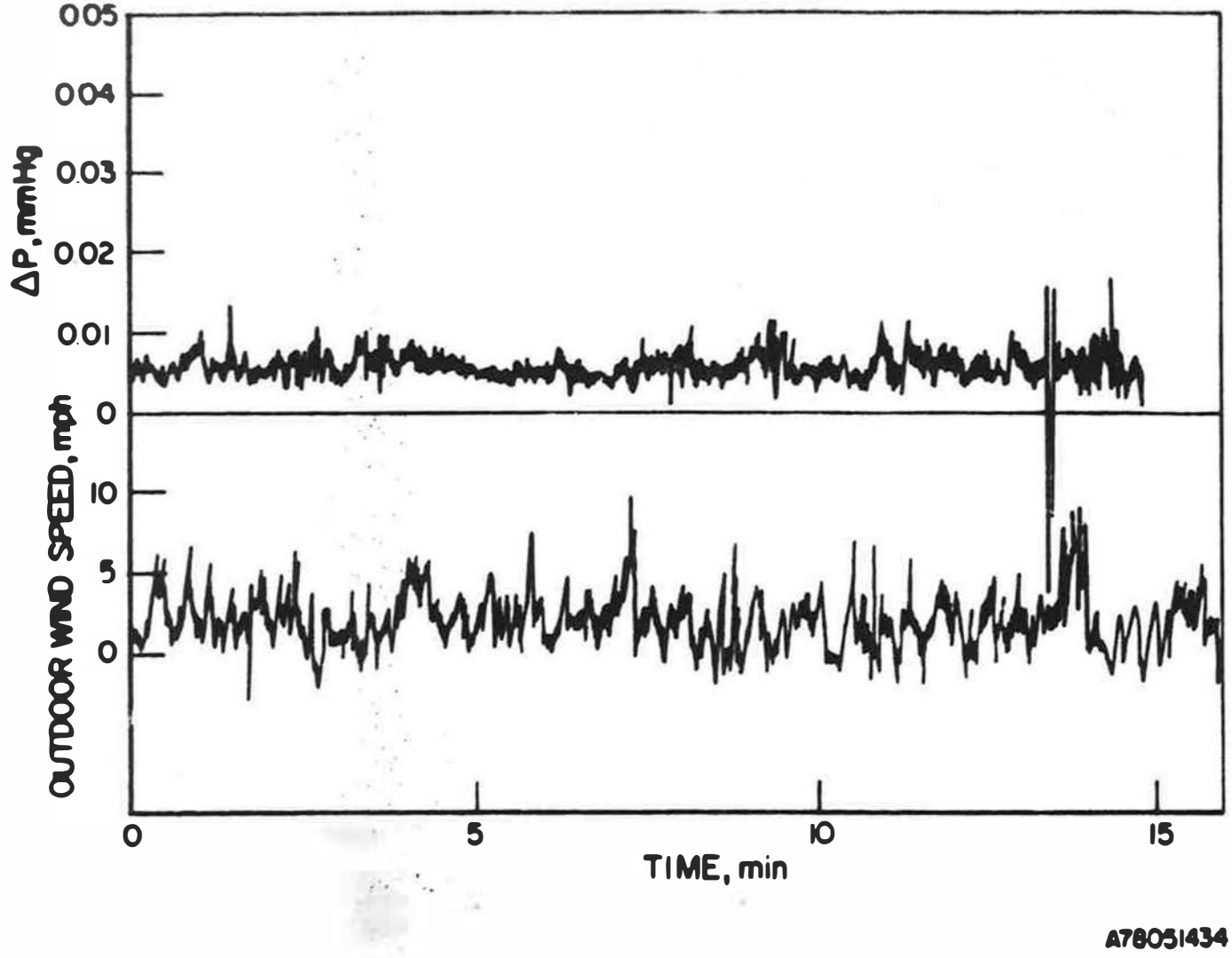

Figure 25. PRESSURE DIFFERENTIAL MEASUREMENTS WITH PROBE IN ATTIC

method with the direct method due to the large variations obtained when using the direct method.

2. Experimental Data

The data from the 8 test homes are shown plotted in an identical manner as a function of structure height above the furnace, in Figures 26 through 33. The indoor-outdoor pressure differential profiles for each home are shown for 3 cases: furnace off, stack closed; furnace off, stack open; and furnace on, stack open. The profiles, in general, behave in a manner similar to the calculated profile discussed earlier (i.e., the pressure differential increases linearly with height).

The effect of opening the stack is best demonstrated with the data obtained from Test Home No. 8, summarized in Figure 26. With the stack closed, the indoor-outdoor pressure difference (ΔP_x) was found to be positive at each level above the furnace level, while the structure was being subjected to a wind from the west at 17 mph, at an outdoor temperature of 55°F, during the course of the measurements. The ΔP_x was found to vary from +0.001 to +0.008 in. H_2O, which translates to an indoor pressure higher than the static outdoor pressure at every level of the house.

Figure 26 also shows that, when the stack was opened, the pressure in the house became entirely negative with respect to the outside, ranging from − 0.008 to − 0.032 in. H_2O, with the pressure differential at each height reduced by 0.008 in. H_2O. This behavior is qualitatively consistent with the notion that opening the stack increased significantly the crackage for exfiltration; the existing buoyant forces created additional flow (up the stack) and, therefore, caused an increase in the rate of infiltration to satisfy the mass balance around the house. Indeed, the measured infiltration rate, with the stack open (0.51 air changes/hr), was found to be much greater than with the stack closed (0.33 air changes/hr). On the other hand, quantitative correlation between ΔP_x, the infiltration increase, the wind speed and indoor-outdoor difference, the relative crackage of the house, the wind direction, etc., has not yet been established because of the absence of a comprehensive and interactive governing model, which is presently under development.

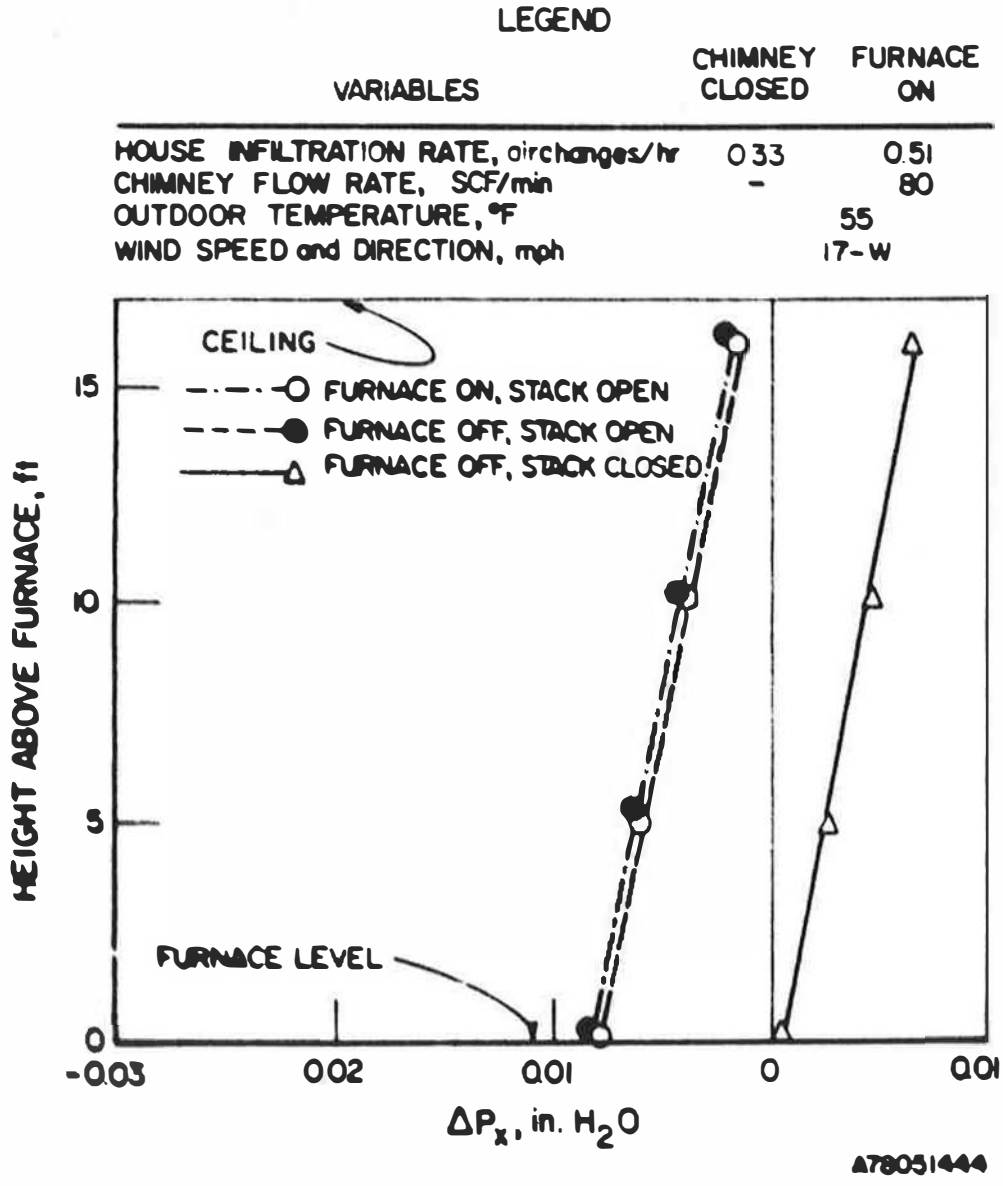

Figure 26. INDOOR-OUTDOOR PRESSURE DIFFERENTIAL MEASUREMENTS IN HOUSE NO. 8 (Vavrik)

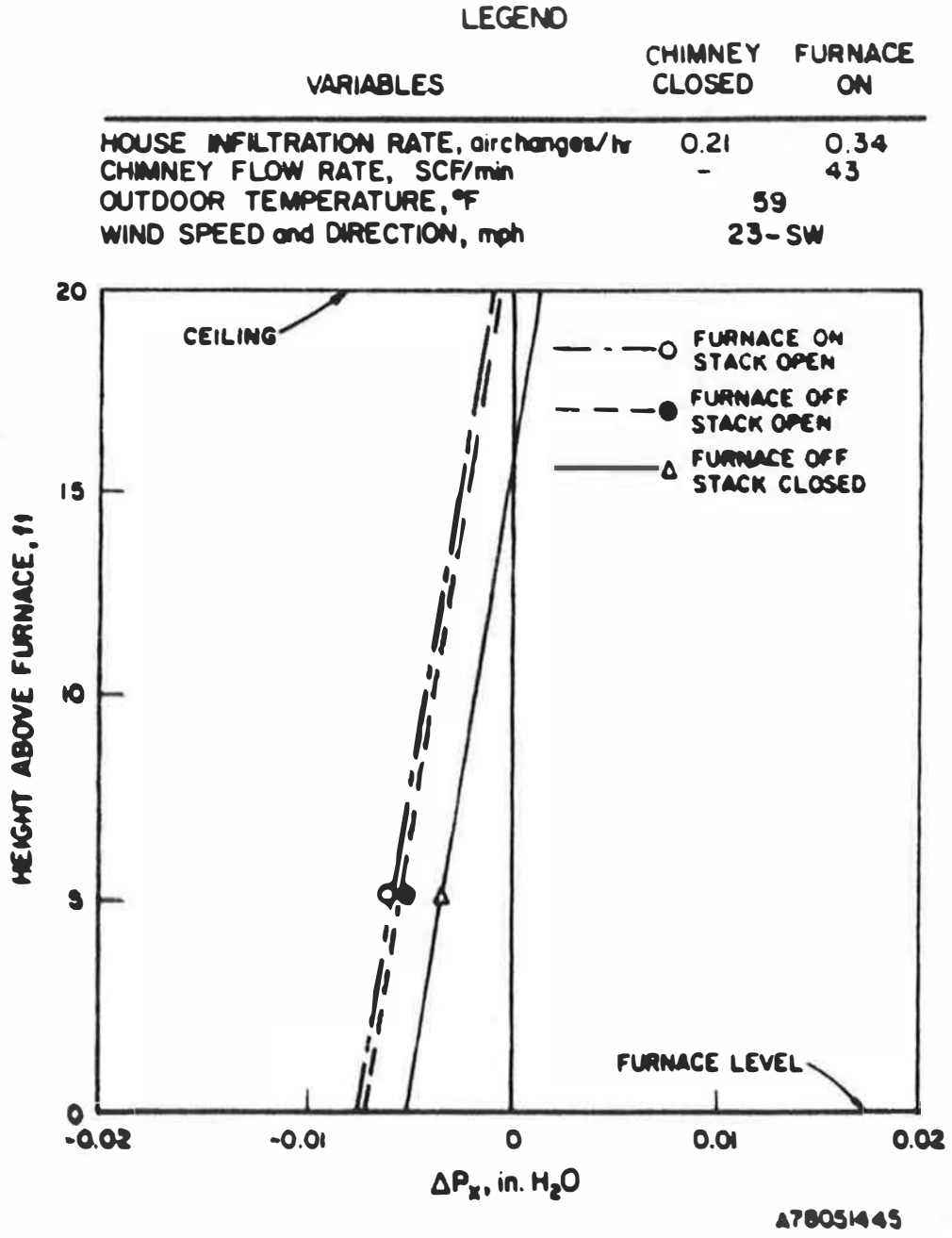

Figure 27. INDOOR-OUTDOOR PRESSURE DIFFERENTIAL MEASUREMENTS IN HOUSE NO. 43 (Patterman)

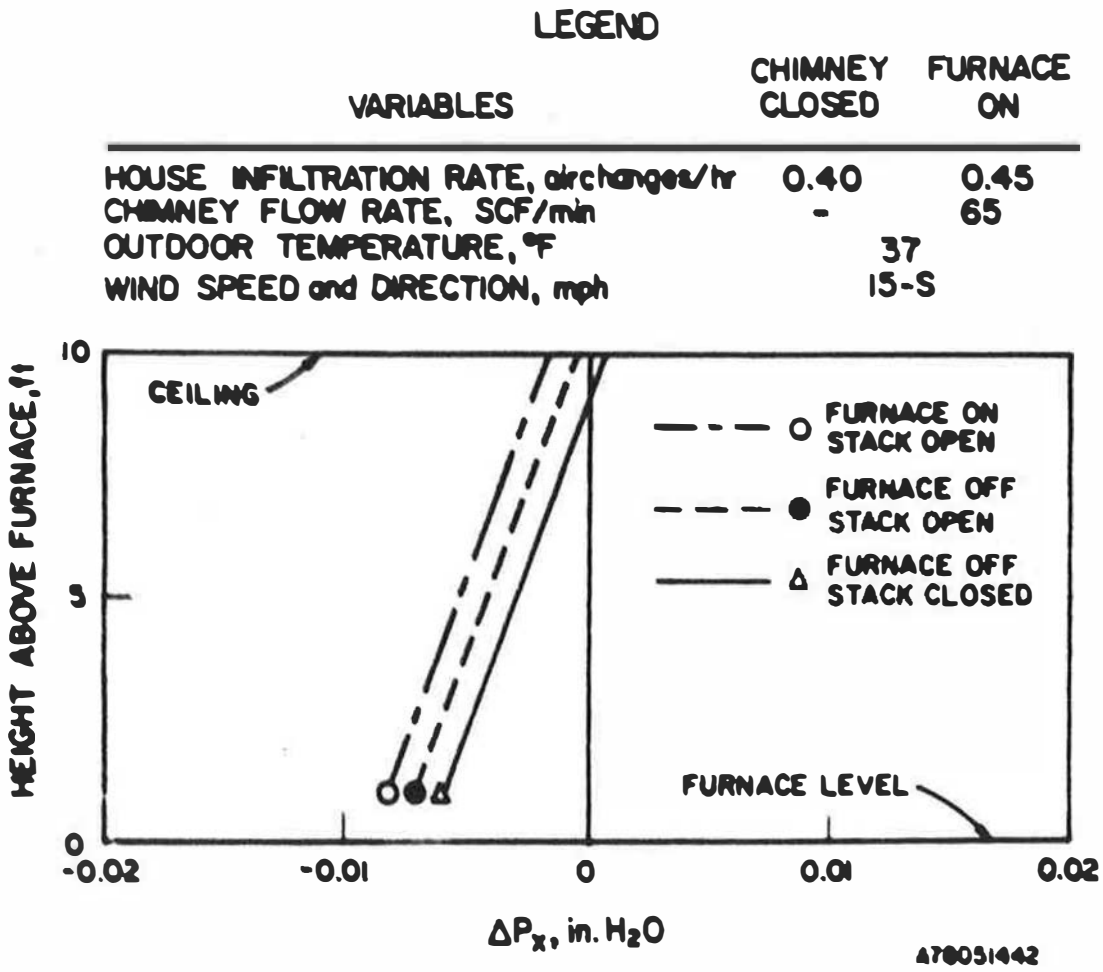

Figure 28. INDOOR-OUTDOOR PRESSURE DIFFERENTIAL MEASUREMENTS IN HOUSE NO. 4 (Petrulis)

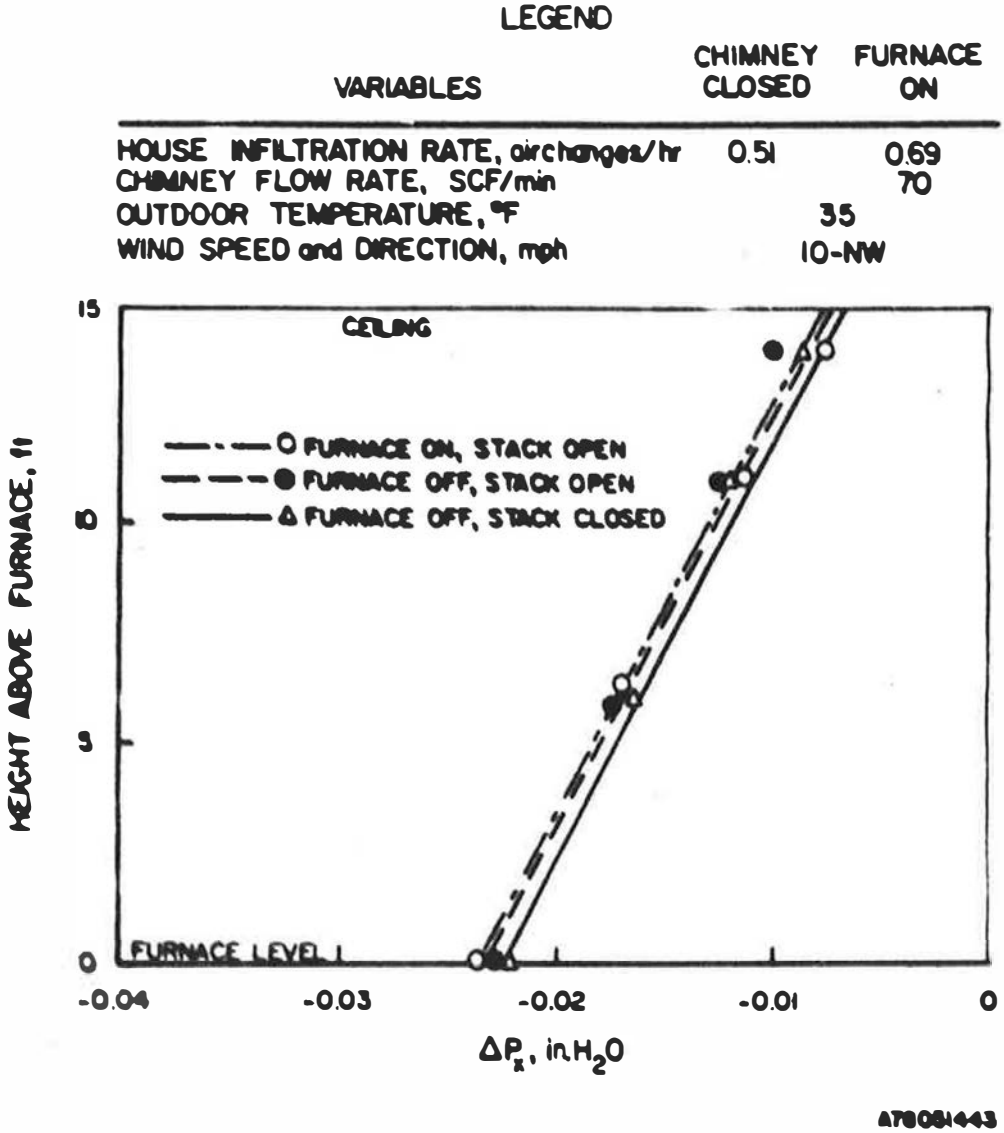

Figure 29. INDOOR-OUTDOOR PRESSURE DIFFERENTIAL MEASUREMENTS IN HOUSE NO. 5 (Soderquist)

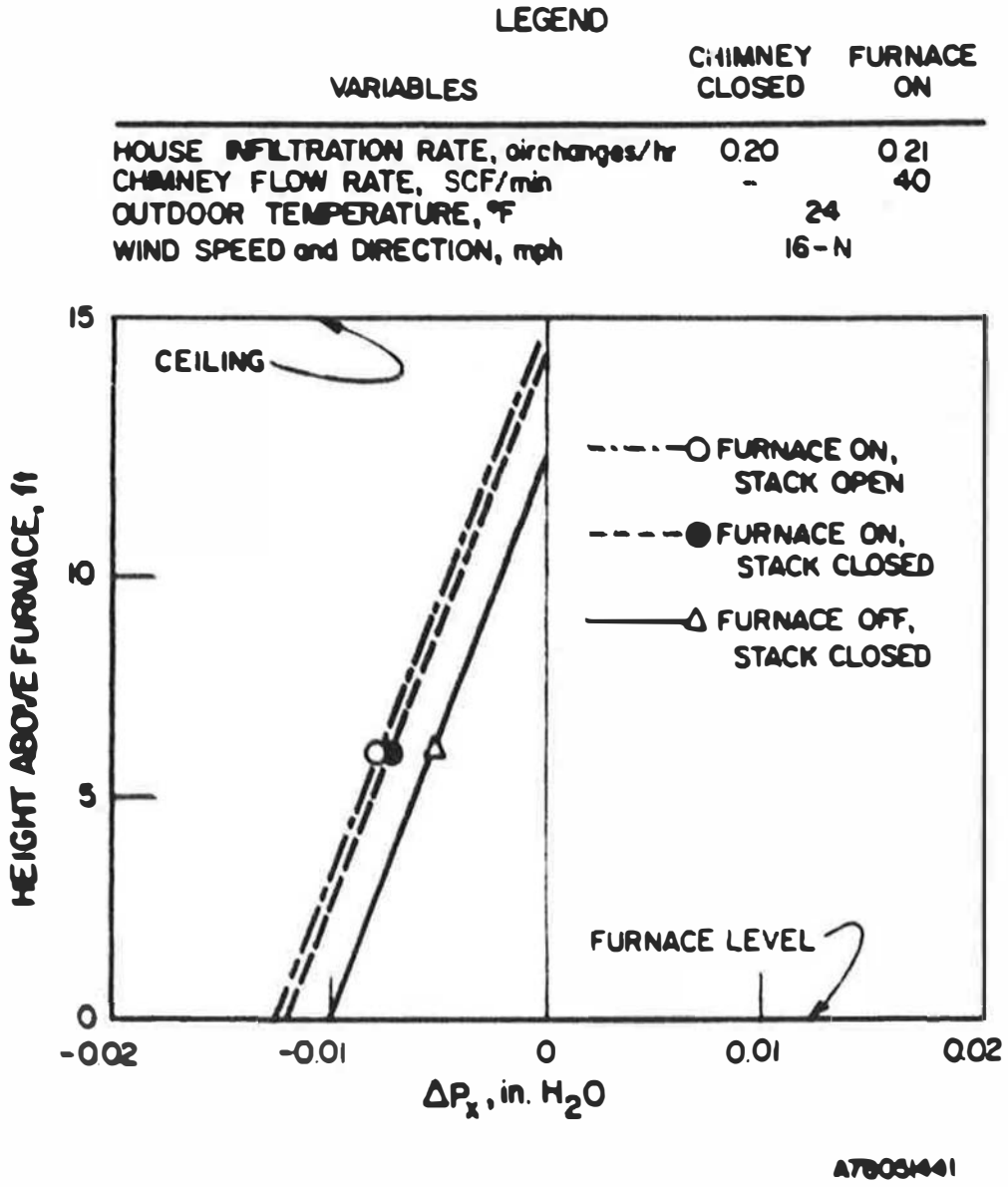

Figure 30. INDOOR-OUTDOOR PRESSURE DIFFERENTIAL MEASUREMENTS IN HOUSE NO. 42 (Weber)

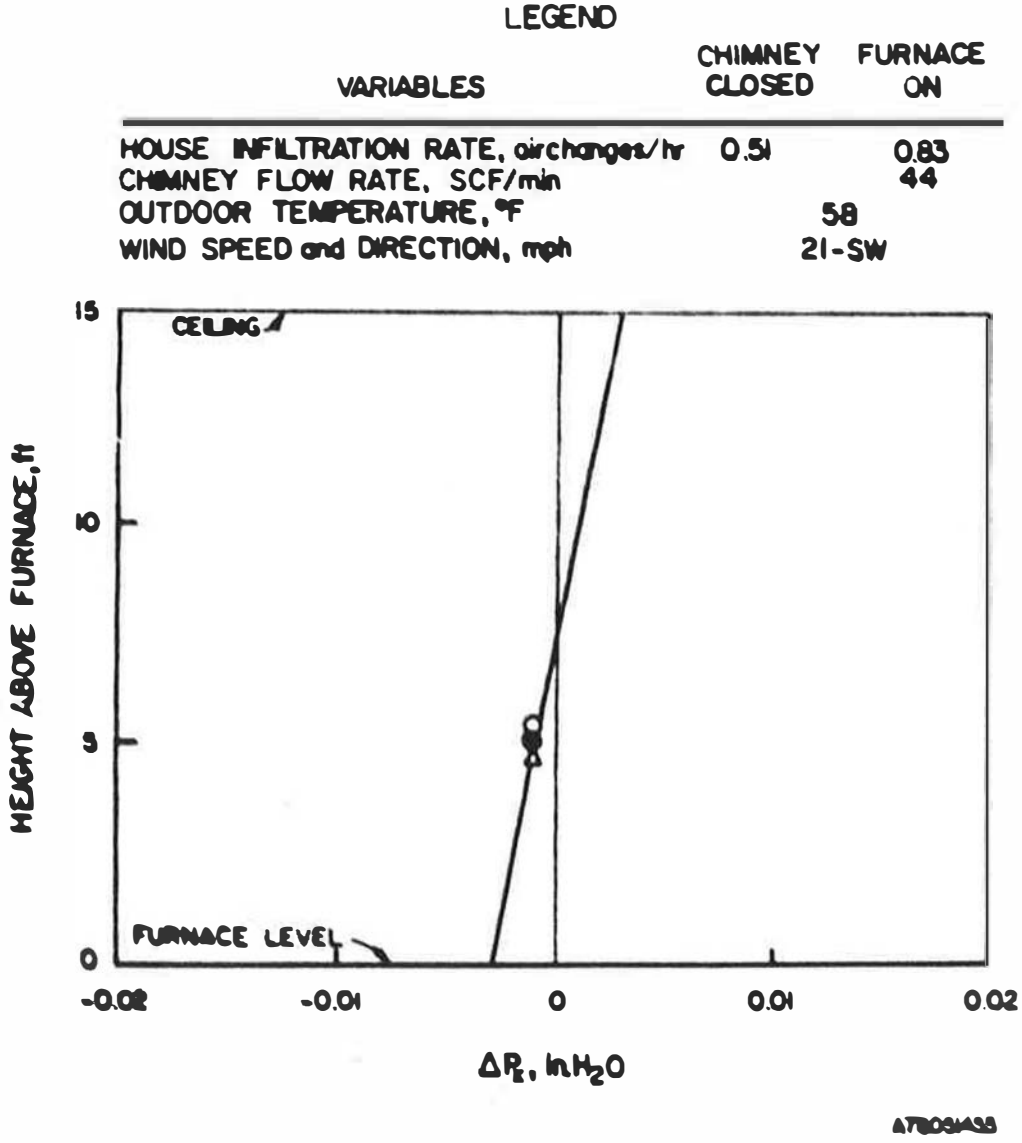

Figure 31. INDOOR-OUTDOOR PRESSURE DIFFERENTIAL MEASUREMENTS IN HOUSE NO. 40 (Hexdal)

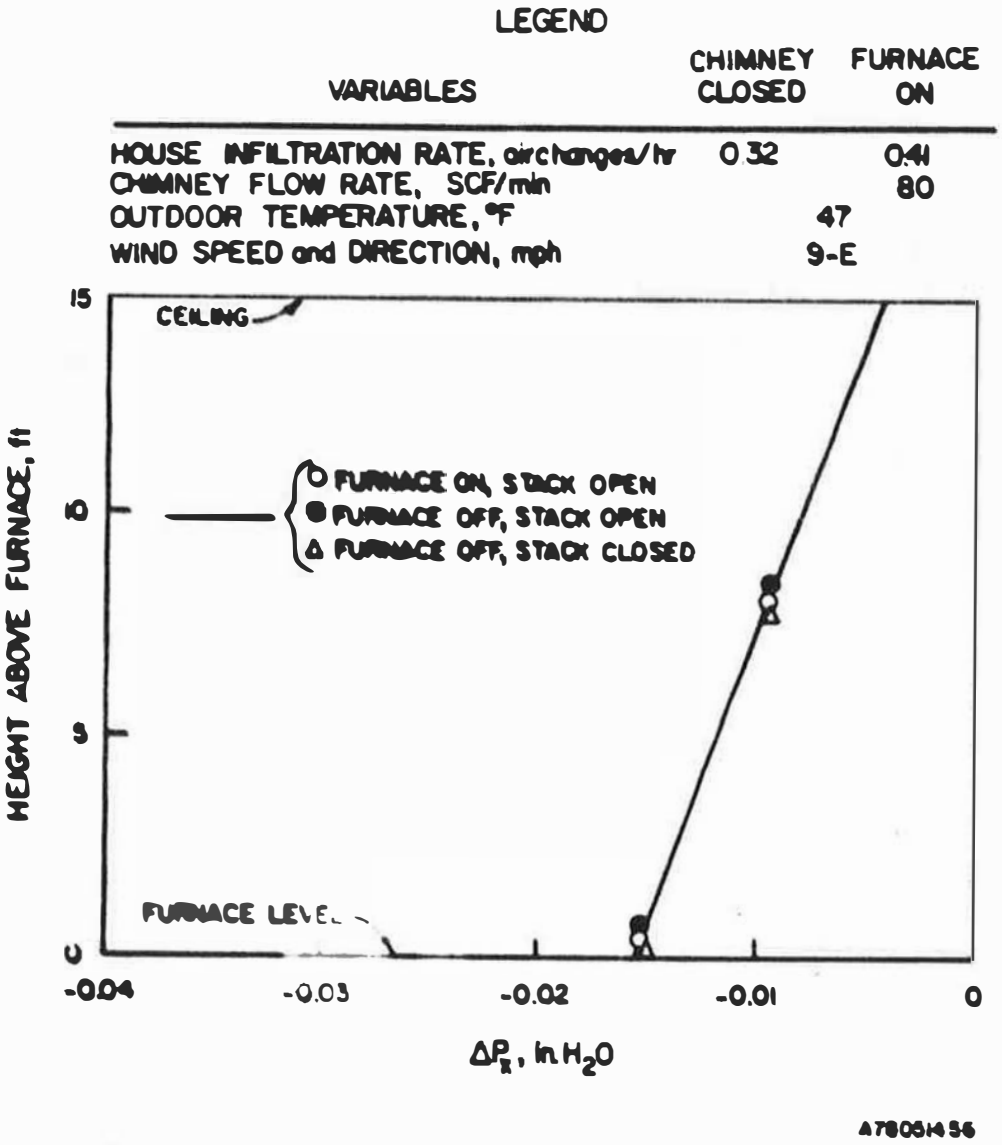

Figure 32. INDOOR-OUTDOOR PRESSURE DIFFERENTIAL MEASUREMENTS IN HOUSE NO. 46 (Elliott)

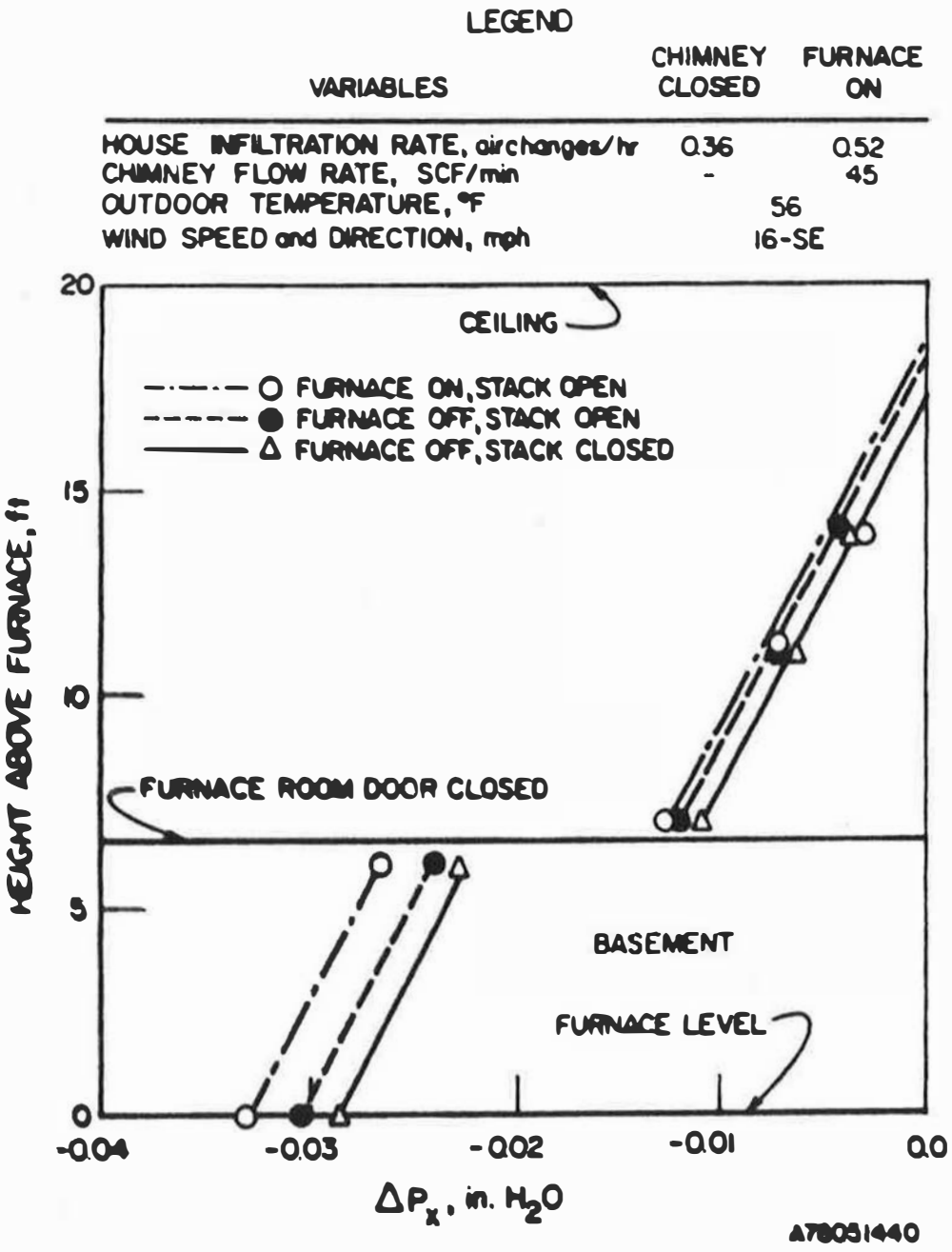

Figure 33. INDOOR-OUTDOOR PRESSURE DIFFERENTIAL MEASUREMENTS IN HOUSE NO. 6 (Ingemanson)

Figure 26 also shows that furnace operation, at steady state, further decreases the pressure in the house -- a fact consistent with the increase in the buoyant force due to the hot flue products. Figures 27 through 30 present the data for Test Home Nos. 43, 4, 5, and 42, respectively. In these test homes, the general behavior observed with Test Home No. 8 is repeated, with two exceptions: the level of pressure reduction upon opening the stack (which varies from one home to the other) and the initial ΔP_x (with the stack closed). In each of these 4 homes, the initial ΔP_x was found to be mostly negative, despite the fact that the wind speed levels (and directions) were 23-SW, 15-S, 10-NW, and 16-N, respectively. Again, quantitative relationships to explain these behaviors are not available at this time, and the data are presently being analyzed to aid in the model development. An even more difficult behavior is presented with the following two test homes, Nos. 40 and 46 (Figures 31 and 32), in which no change in the ΔP_x was observed (whether the stack was open or closed or the furnace burner was on or off) while appreciable changes in the air infiltration rates were recorded.

Test Home No. 6 (Figure 33) represents a special case: In this home, the door to the furnace room was kept closed during the ΔP_x measurements, and, as a result, a discontinuity was observed in the pressure levels between the furnace room and the rest of the house. Above the furnace room (basement), opening the stack caused only a small shift (0.001 in H_2O) in the pressure profile. However, in the furnace room, there were noticeable effects on the pressure profile when opening the stack and operating the furnace. The large pressure drop (0.012 in. H_2O) observed across the furnace room door suggests that the sealing of the two zones was such that flow was established through the door crack to the basement. Because the furnace air fan was operating continuously, air from the basement was drawn into the return air plenum of the furnace and finally discharged upstairs. This postulate explains fully the change in pressure upstairs as a function of any action along the chimney.

THE IGT MODEL AND COMPUTER PROGRAM

The ideal air infiltration model would be one for which all of the parameters used can be defined numerically from the appropriate weather data and the detail architectural drawings of the structure. As discussed earlier, Hittman Associates[8] have moved in this direction by using an equivalent orifice coefficient, which presumably can be estimated from measurable characteristics of the structure. This approach attempts to define an "average" driving force, ΔP, acting simultaneously on all the orifices in the house, in terms of a static relationship with wind speed, wind direction, indoor-outdoor temperature difference, and other factors such as furnace and/or fan operation as parameters. Such an "average" driving force, however, does not reflect the effects of the interactions between the driving forces over a broad range of ambient conditions, and, therefore, does not provide an accurate basis for predicting infiltration for variable structures, in variable environments.

In reality, the driving force, ΔP, acting on a particular orifice varies widely depending on its location with respect to wind direction and height of the house. The actual pressure drop, ΔP, across a particular orifice is determined by the difference between the dynamic pressure on the outside of the orifice imposed by wind forces, ΔP_w (for which a reasonable model exists), and the resultant indoor-outdoor static pressure difference, ΔP_r:

$$\Delta P = \Delta P_w - \Delta P_r \qquad (23)$$

where ΔP_r is the sum of two indoor-outdoor static pressure difference effects.

One of these pressure differences is ΔP_B, the static pressure difference at a particular height in the house, resulting from the vertical gradient induced by the indoor-outdoor temperature difference only. Its value may be estimated from the indoor-outdoor temperature difference, ΔT, and the height of the orifice above or below the structure's neutral zone. The other is ΔP_X, the static pressure difference induced by the combined effects of wind, chimney buoyancy, and fan forces (at mass balance). The pressure difference, ΔP_X, affects the whole house equally, depending on communication between rooms and between floors.

We can, therefore, define the flow, F, through a particular orifice in terms of the following equation:

$$F = OC\ [\Delta P_w - (\Delta P_B + \Delta P_x)]^n \qquad (24)$$

where OC is the measurable orifice coefficient for the particular orifice. All of the parameters in Equation 21 are calculable or measurable except the flow, F, through the orifice and ΔP_x. The latter can be determined by mass balance between the exfiltration and infiltration through all of the orifices in the house. It is possible, therefore, to compute the whole house static pressure difference, ΔP_x, as well as the overall infiltration rate, by characterizing all of the orifices in the house in terms of Equation 24 and by setting up an overall mass balance equation for infiltration-exfiltration through all orifices. Such an equation can then be solved by the method of successive approximations.

In order to successfully model a house in terms of such mass balance equations, the following are required:

- Indentification and characterization (in terms of the orifice coefficient and location with respect to which wall and height) of all significant components in the house through which infiltration can occur.

- Estimation of the "base-line" neutral zone height, h_{no}, in the absence of wind, chimney, and exhaust-fan forces. Presumably this can be obtained from the vertical gradient in the measured orifice coefficients. From this, and the given indoor-outdoor temperature difference the induced pressure difference, ΔP_B, at any location can be calculated as follows:

$$\Delta P_B = (0.26)(h-h_{no})\ \Delta R\left(\frac{1}{T_i} - \frac{1}{T_o}\right) \qquad (25)$$

where T_i and T_o are indoor and outdoor temperatures, respectively.

- Appropriate models for calculating the actual wind pressures imposed on each of the four walls of a structure, from remote and on-site wind measurements. Precise modeling of the aerodynamic interactions between wind, a particular structure, and the shielding effect of planting and other structures is complex and beyond the scope of this project. However, models available from ASHRAE are probably adequate for our purposes.

- Appropriate models for exhaust fan and chimney flow, which are also available.

Pressure differentials usually exist across the walls of building structures and are caused by

- The density difference between the warm indoor and colder outdoor air
- The effect of wind forces.

In the absence of wind, a neutral pressure point is found somewhere within the structure, and infiltration of outside air occurs through that part of the structure physically located below the neutral zone, with exfiltration occurring above it, as shown in Figure 1. The exact height (Y) of the neutral zone is dependent upon the relative permeability of the structural members (solid walls, windows, and doors), which usually causes the compound walls of the structure to have variable overall permeability.

A. Preliminary Assumptions

For the "basic" model of air infiltration, we have assumed (for simplicity) that the vertical gradient in permeability is uniform, and can be varied wall-by-wall. This wall-by-wall mass balance model excludes the added interactive effects of furnace operation which represent the final refinement of the model. With these assumptions, we can now examine how the representation of Figure 34 (for neutral pressure zone) is changing when the outdoor conditions change.

First, if the indoor-outdoor temperature difference increases, the pressure differential indicated by the slope of the line passing through the neutral zone will increase, thereby causing a greater flow through the cracks in walls, windows, etc. Also, in the absence of wind, the neutral pressure zone position (height) should be the same on all four walls of the structure (uniform vertical permeability gradient). On the other hand, addition of wind forces will be defined, one on the windward, the other on the leeward wall. These zones will be positioned such that there is a mass balance between air infiltration and exfiltration. The difference in the height of the neutral zone position (Z) is proportional to the ratio of the wind speed force to the buoyant force.

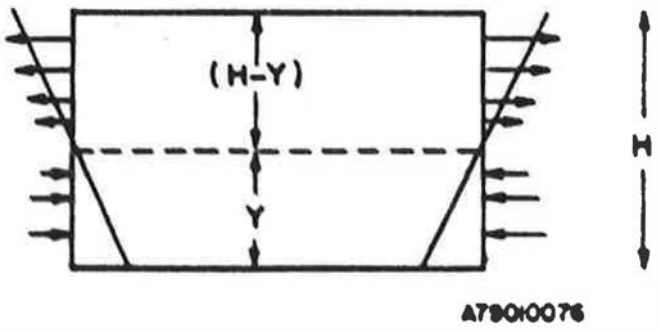

Figure 34. INFILTRATION AND EXFILTRATION UNDER NONWIND

With regard to the usual levels of wind velocities and indoor-outdoor temperature differences characteristic of the four seasons, at least four distinct representations can be envisioned (based on the assumptions made above) for the neutral zone position for air infiltration to occur. Figure 35 shows the case when the absolute level of wind, the indoor-outdoor temperature difference, and the relative wall permeability are such that both the windward and leeward neutral zones are within the structure.

Similarly, Figure 36 illustrates the case when the windward wall zone is above the structure and the leeward wall neutral zone is within the structure. Figure 37, on the other hand, shows the reverse case (windward zone within and leeward zone without the structure) and Figure 38 the case when both zones are outside the structure. It is the object of the modeling effort to provide a tool that would allow the determination of the exact locations of the neutral zone in each case (and, therefore, of the rate of infiltration) by using the basic properties of the structure and specific weather data.

For each case shown in Figures 35 through 38, the mass balance formulations around the structure were obtained by equating infiltration and exfiltration above and below the neutral zone. Each such formulation represents a complex non-linear mass balance equation and the following simplifying assumptions were necessary in order to obtain the required solutions:

- The pattern of crackage is uniform across a wall
- The air flow through a crack is proportional to the 0.50 power of the air pressure differential
- The wind pressure force on the windward walls is positive and does not cause any pressure disturbances on the other walls
- For winds that are not perpendicular to a wall of the house, the wind pressure effect is the cosine of the wind angle (with respect to the walls it acts upon) times the wind speed squared
- The house is considered without a chimney and exhaust fan force (these effects will be added in the final, refined model).

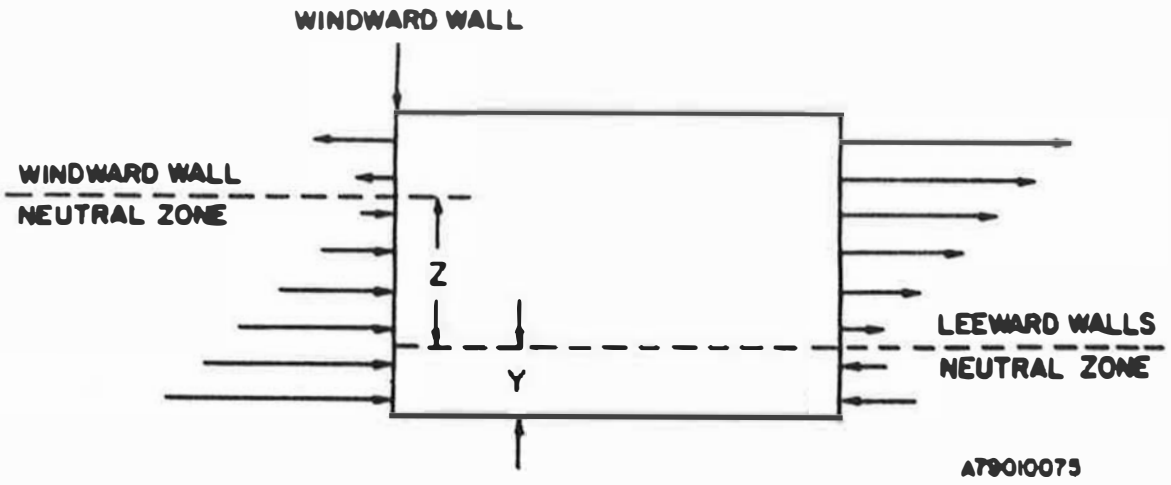

Figure 35. BOTH WINDWARD AND LEEWARD WALL NEUTRAL ZONES INSIDE THE HOUSE

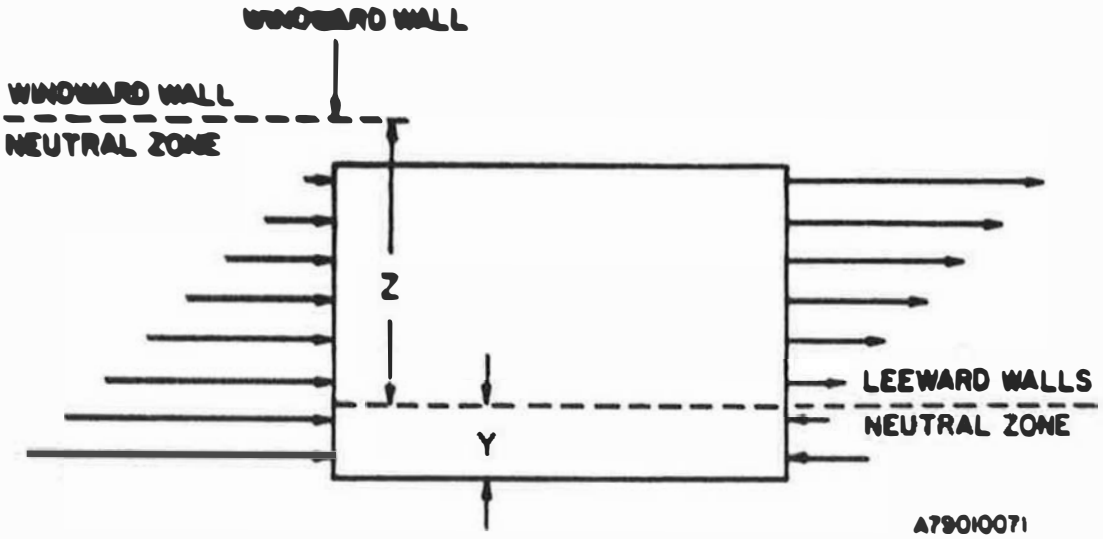

Figure 36. WINDWARD WALL NEUTRAL ZONE ABOVE HOUSE LEEWARD WALL NEUTRAL ZONE INSIDE HOUSE

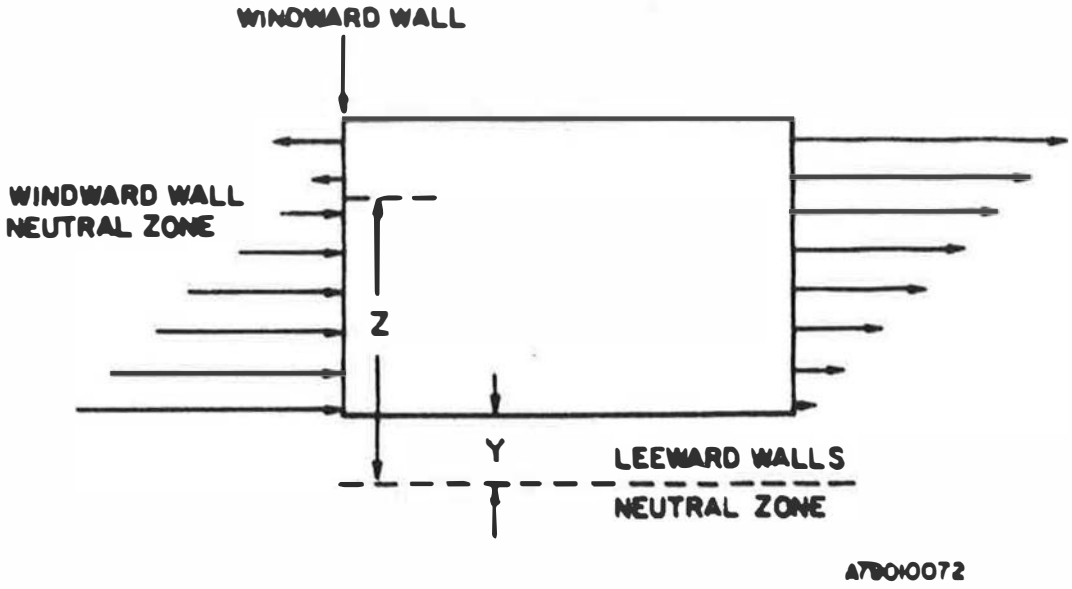

Figure 37. WINDWARD WALL NEUTRAL ZONE INSIDE HOUSE LEEWARD WALL NEUTRAL ZONE BELOW HOUSE

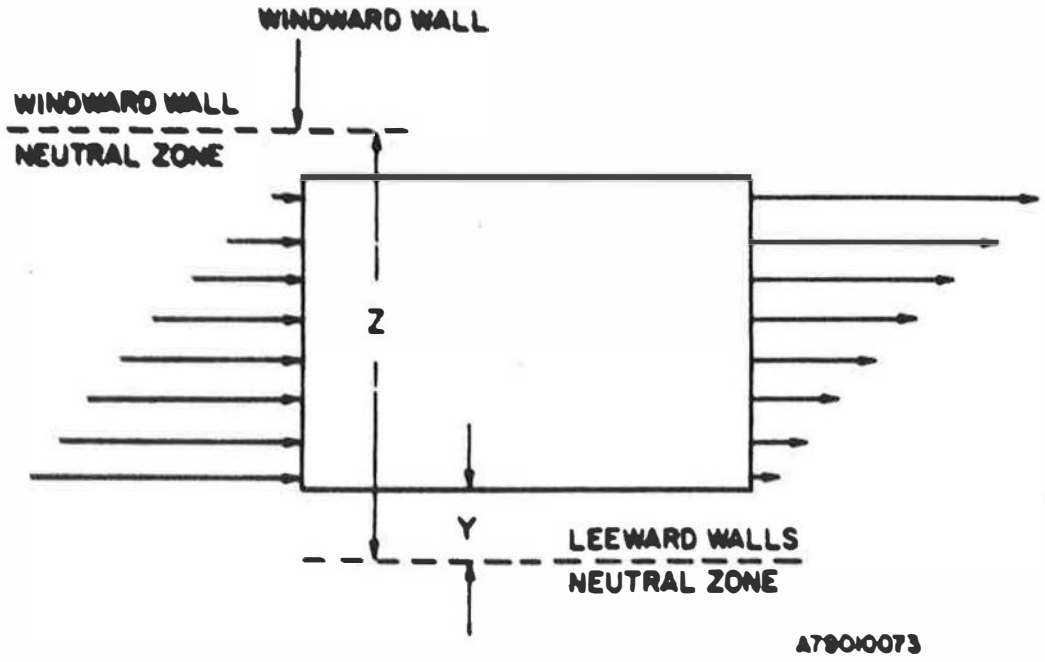

Figure 38. BOTH WINDWARD AND LEEWARD NEUTRAL ZONES OUTSIDE THE HOUSE

b. Input Data Requirements

A computer program has been developed to facilitate the solution of the mass balance equations for the four cases mentioned earlier and was also used to provide a measure of validation of the model using data from the IGT field test homes.[21]

The data required to perform the mass balance model calculations include the following:

- The height of the house
- The crackage length of the windward wall(s), and of the leeward walls
- The indoor and outdoor temperatures
- The wind speed and direction.

As the simplified "basic" model is refined, additional data concerning furnace operation, vent-fan operation, and ground wind or structure shielding will be added to the above data.

The program first computes the magnitude of Z (the difference in the height of the neutral zone) and then compares the magnitude of Y (neutral zone height) for each wall against the structure's height (H), in order to define the appropriate case Figures 35 through 38) and respective mass balance equation applicable. This program proceeds to set a value for Y for the leeward wall(s) at its lowest limit possible and to increase this value progressively, in small increments, until the mass balance between infiltration and exfiltration is satisfied. The output, then, of the program is the height of the neutral pressure zone on the leeward wall(s) from ground level. Using this value of Y an estimate of the equivalent wall permeability is obtained, using the actual infiltration data for the structure and measured cracked lengths.

As will be discussed later, the above permeability values are compared with values from the literature relative to the types of homes used in the program in order to provide model verification. Conversely, permeability data from the literature and the actually measured crack-length data can be

input to the program to estimate the structures infiltration. This latter approach has not been used for data from the literature, due to absence of actual infiltration data, and has only been used for the IGT homes and measured infiltration rates for these homes.

VALIDATION OF THE BASIC MODEL

Validation of the model against field data not only requires that the model itself be valid in form, but also in content (i.e., the input house parameters and on-site weather data must be valid). Therefore, although we know that the mass balance model is basically sound, a lack of agreement of measured field data with model predictions can occur due to a number of factors. In the first place, the model in its present form assumes a uniform vertical permeability gradient whereas, in real houses, the sites of infiltration occur as more or less discrete components and the vertical gradient in permeability is undoubtedly non-uniform.

For conditions such that the driving force for infiltration is either buoyancy (indoor-outdoor temperature difference) or wind, the above assumption should have little effect on the results obtained with the model. However, when both are present, the assumption of uniform permeability could effect the ratio of wind speed to the temperature difference at which transition from one predominant regime to another occurs, since the neutral zone height is determined by the vertical gradient.

Other factors that could effect the agreement between model predictions and data from the field are:

- Imprecise determinations of the location and magnitudes of the permeability coefficients for exfiltration (K_x) and infiltration (K_i)
- Improper assignment of the wind pressure exerted on the various walls of the house, the result of "shielding" and aerodynamic interaction of the wind with structure, which are not taken into consideration in the preliminary form of the "basic" model.

Because of the above, validation of the model against field data requires agreement in the magnitude of infiltration as well as consistency over a wide range of weather parameters.

A. Comparison With Chimneyless Homes

We have used the data obtained from 19 field homes ("extensive" testing), for the weather conditions existing during the period of the measurements (with the chimney blocked) to compare with estimates for these homes obtained with the model and computer program. Similarly, we have used data obtained from the ranch home ("intensive" testing) for the same purpose.

1. Comparisons With Field Data

For the 19 field homes, we have used the measured crack lengths, air infiltration rates, and height of living area as the sole inputs to the program. The comparative results are summarized in Table 6.

In this table, the comparisons are made in terms of the orifice coefficient (cubic feet of air per minute per foot of window and door crackage and inch of water pressure) required to make the measured and calculated infiltrations agree. This, in essence, attributes the infiltration from building elements (such as sill plate crackage, wall leakage, electrical outlets, and ceiling leakage) which are poorly characterized to the window and door crackages which can be characterized. Therefore, to the extent that the window and door crackages in a house can be characterized, the orifice coefficients so calculated are measures of the relative contribution of other orifices to the total infiltration.

Current ASHRAE data[2] indicate that orifice coefficients for wooden double hung windows vary from 0.9 for average fit, weather-stripped condition, to 1.7 for average fit, non-weather-stripped windows. With storm windows, these values would be reduced by about 30%, to 0.64 to 1.2. Window-frame-wall leakage, which is additive with the window leakage values, may vary from 0.3 to 0.9. Orifice coefficients for doors are likely to be about double those for the windows and, therefore, typical orifice coefficients for total window and door crackage (with storms) in real homes might be expected to be in the range of 0.6 to 3.0 cubic feet per minute per foot and inch of H_2O.

Tamura[18] found in 6 real homes (Toronto) values ranging from 0.6 to 2.7 for double hung windows with storms, and 1.0 to 2.5 for doors with storms. Thus, the range from 0.6 to 3.0 seems reasonably typical for comparative purposes.

The data of Table 6 show that the calculated orifice coefficients varied from 0.7 (indicating a very tight house) to as much as 27. For one-half (27 of 54) of the measurements, however, the calculated orifice coefficients were in the range of 0.7 to 3.0. Even more, only 11% (6 of 54) of the calculated coefficients were above 6.0 and these appear to be spurious results.

Table 6. CALCULATED ORIFICE COEFFICIENTS FROM MEASURED INFILTRATION DATA

House Number	WS MPH	ΔT °F	K_x/K_1	Measured Infiltration CFM	Control Regime Figure	Orifice Coefficient, CFM / Ft, in H_2O
2	9	14	1.1	130	5	2.8
	10	24	2.5	120	5	3.2
4	18	26	1.1	268	5	7.1
	7	17	2.9	185	5	16.1
	15	31	1.1	123	5	3.9
5	12	17	0.8	101	5	2.8
	14	9	19.1	95	5	14.7
	30	67	1.1	353	5	3.8
	10	33	1.1	152	5	5.0
6	9	22	2.3	80	5	3.1
	14	9	1.2	98	5	2.1
	17	31	1.1	178	5	3.2
	16	32	0.6	110	5	2.6
7	9	1	1.1	128	5	3.4
	11	1	1.1	250	5	5.5
	16	7	999	246	5	25.8
	10	43	1.1	141	5	2.9
8	5	2	999	40	5	15.9
	8	10	999	79	5	13.8
	19	65	1.3	249	5	4.0
	17	11	1.3	81	5	1.4
9	16	23	9.6	66	5	4.7
	15	10	1.0	61	5	1.6
	19	35	9.6	89	5	5.2
12	9	8	0.9	108	5	2.7
	11	1	0.9	125	5	2.6
13	12	1	3.3	94	5	3.0
	15	1	999	84	5	14.8
	3	31	3.3	134	5	6.0
	10	62	3.3	172	5	4.9
23	10	27	3.1	102	5	3.7
24	16	9	3.6	39	5	0.9

Table 6, Cont. CALCULATED ORIFICE COEFFICIENTS FROM MEASURED INFILTRATION DATA

House Number	WS MPH	ΔT °F	K_x/K_i	Measured Infiltration CFM	Control Regime Figure	Orifice Coefficient, CFM / Ft, in H_2O
32	14	32	2.5	116	5	2.4
	18	5	2.7	143	5	3.0
	18	36	0.5	132	5	2.5
	10	48	2.5	141	5	4.0
39	8	42	0.9	163	5	5.6
	17	35	0.9	287	5	4.3
	13	47	1.3	241	5	5.0
40	12	27	2.3	40	5	1.6
	14	21	2.3	40	5	1.4
	10	34	2.3	34	5	1.7
41	8	2	4.8	54	5	1.4
42	21	31	0.9	59	5	0.8
	8	3	1.9	21	5	0.7
43	23	13	0.9	96	5	1.4
	8	33	1.8	75	5	3.3
	10	29	1.8	88	5	3.4
F0	19	28	1.7	78	5	1.4
	13	31	1.7	92	5	2.4
	18	31	2.7	89	5	1.3
F1	1	23	1.0	24	5	2.0
	16	37	0.6	53	5	1.0
	8	36	0.6	53	5	1.9

The data of Table 6 show that the values of the orifice coefficients are very consistent over a fairly broad range of ambient conditions in many of the homes (house numbers 6, 12, 43, 2, F0, F1, 39, 32, 40, and 42), whereas in others (9, 4, 5, 13, 8, and 7) we note significant deviations at different weather conditions. These latter discrepancies are noticed primarily when the model calculation refers to the interactive model (Figure 3) and, particularly, at relatively high values of the K_x/K_i ratio.

Specifically, the inconsistent values obtained for houses 5, 7, 8, and 13 (all of the interactive model case) are for exceptionally high value of K_x/K_i (19 and 999). A more realistic assignment of the K_x/K_i values would, probably, provide fully consistent comparisons between model and measurements. For house number 9, the two values obtained relative to the interactive model case at K_x/K_i equal of 9.6 are significantly higher than the values obtained for the model case of Figure 5 at K_x/K_i of 23.

For house number 4, the discrepancies exist for the values within a model case (Figure 3) and between model cases (Figures 3 and 5). This has been identified to be due to exceptionally high supply air duct leakage (of the same magnitude as the infiltration rates measured) which are incurred during blower operation. Therefore, in house number 4, the infiltration is dominated by duct losses which are unrelated to the ambient conditions.

Table 7 summarizes the calculated orifice coefficients and other descriptive data for four different types of building structures:

- Full 2 story with basement
- Split levels
- One story with basement
- One story on slab.

Table 7 shows that the average orifice coefficient for the one story homes, as well as the individual coefficients for all but two of the homes, is well within the range of tight window and door crackage coefficients. (The significantly greater than average value for house number 5 is in part due to the lack of storms.) These results suggest that the major fraction of the infiltration in these one-story homes is, in fact, due to window and

Table 7. CALCULATED ORIFICE COEFFICIENTS FOR DIFFERENT RESIDENTIAL TYPES

Full 2-Story Homes With Basement

House Number	Age	Type of Construction	Size ft^2	Calculated Orifice Coefficients CFM/ft/in H_2O		Other Comments
				Ave.	Lowest Value	
7	6	F	2000	3.9	2.9	Fireplace
39	2	F	2100	4.7	4.3	Fireplace
23	13	F	3000	3.7	3.7	Fireplace
2	50	F	2100	3.0	2.8	Fireplace
13	30	B	1250	3.0	3.0	Fireplace
AVERAGE				3.7	3.4	
		Split Levels				
F0	22	B, F	1800	1.7	1.3	Almost Identical Structures
F1	22	B/F	1800	1.5	1.0	
12	4	F	3800	2.6	2.6	Duct Losses
8	18	F	2500	2.7	1.4	
43	18	B	2200	2.4	1.4	
6	11	B/F	2000	2.8	2.1	
AVERAGE				2.3	1.8	

Table 7, Cont. CALCULATED ORIFICE COEFFICIENTS FOR DIFFERENT RESIDENTIAL TYPES

1-Story With Basement

House Number	Age	Type of Construction	Size ft^2	Calculated Orifice Coefficients CFM/ft/H_2O Ave.	Lowest Value	Other Comments
40	29	F	805	1.6	1.4	
42	21	F	1400	0.8	0.8	Excellent Construction
32	26	B/F	1300	2.6	2.4	Duct losses negligible
41	14	F	1200	1.4	1.4	
[illegible]	5	F	1100	3.9	2.8	No storm windows
AVERAGE				1.0	1.8	

1-Story On Slab

9	21	F	1000	1.6	1.6	
24	14	[illegible]	1000	0.9	0.9	Duct losses negligible
AVERAGE				1.3	1.3	

door crackage. The addition of sill plate crackage to the model would not change these results significantly.

The average orifice coefficient for the split level houses is only incrementally greater than those for the one-story homes and many of the individual values are comparable. Thus, the above tentative conclusion applies to these split homes as well as to one-story homes.

Table 7 also shows that the average as well as individual orifice coefficients for the full two-story with basement homes are significantly greater than for the other homes. Window and door crackage accounts for less than the major fraction of the infiltration in these homes and the reason for this deviation is not completely clear. The wall area to window crack length ratios, in two-story homes, are probably comparable to those in the one-story homes and, therefore, the difference is probably not due to through-the-wall infiltration. The sill plate to window crack length ratio will be smaller in 2-story homes and thus cannot account for the difference.

Based on the above, it would appear that other factors may be important. For example, infiltration tends to occur at joints and mating surfaces such as window and door perimeters, window and door frame, wall joints, and sill plates. It is possible then that joints between first and second floors, and second floor to attic joints, contribute appreciably to infiltration (similar to window frame to wall joints). Also, because of the height difference, the buoyancy induced exfiltration through the electrical outlets to the attic may be a significant factor in these homes.

Another significant factor which emerges is the extent of duct losses incurred due to blower operation. The results from house number 4 were earlier shown to be almost completely dominated by infiltration due to duct losses. Furthermore, house number 12, whose calculated orifice coefficients are among the highest in the split level group, had relatively high duct losses to the garage (this was deemed by the owner as desirable). It may be significant that the low orifice coefficient for house number 24 is associated with negligible duct losses. On the other hand, house number 32, whose coefficient is second highest in the one-story group, also had negligible duct losses.

Another interesting observation is that the age of the structure may also have an effect (Figure 39). This figure shows that the calculated orifice coefficients appear to decrease with age, for about 10 to 15 years, before leveling out (or increasing). It has been suggested that this could reflect the quality of construction in the past few years particularly in tract homes, and the time it takes for the homeowner to rectify the faults left by the contractor. It also may be significant that the house with the lowest calculated orifice coefficient (house number 42) was built by a contractor for his own use, who was proud of the quality of construction and insulation (verified by our own observation).

Finally, the preliminary comparison (of the results obtained with the "basic" mass-balance model with those measured in the field homes) is very encouraging and shows that:

- The orifice coefficients for the window and door crackages calculated by the model are within the range expected and consistent with laboratory measured values
- The differences between the values found in different homes are in fair measure explainable in terms of differences in structural factors and duct losses.

Actually, the results may be better than we had reason to hope for in view of the anticipated problems in precise assignment of values for the K_x/K_i ratios and of the effect of shielding of the wind by foliage and other houses. The K_x/K_i ratio problem, and its effect on the model's control regime, was avoided by eliminating those points (with K_x/K_i ratios in excess of 9.5) which gave obviously spurious results. Furthermore, the shielding problem may have been minimized by the fact that most of the data were taken in winter, when the shielding by foliage is at a minimum. Also, shielding of the windward wall by other structures may be compensated, in part, by aerodynamic effects on the leeward and neutral walls. Such effects are beyond the scope of this phase of the program.

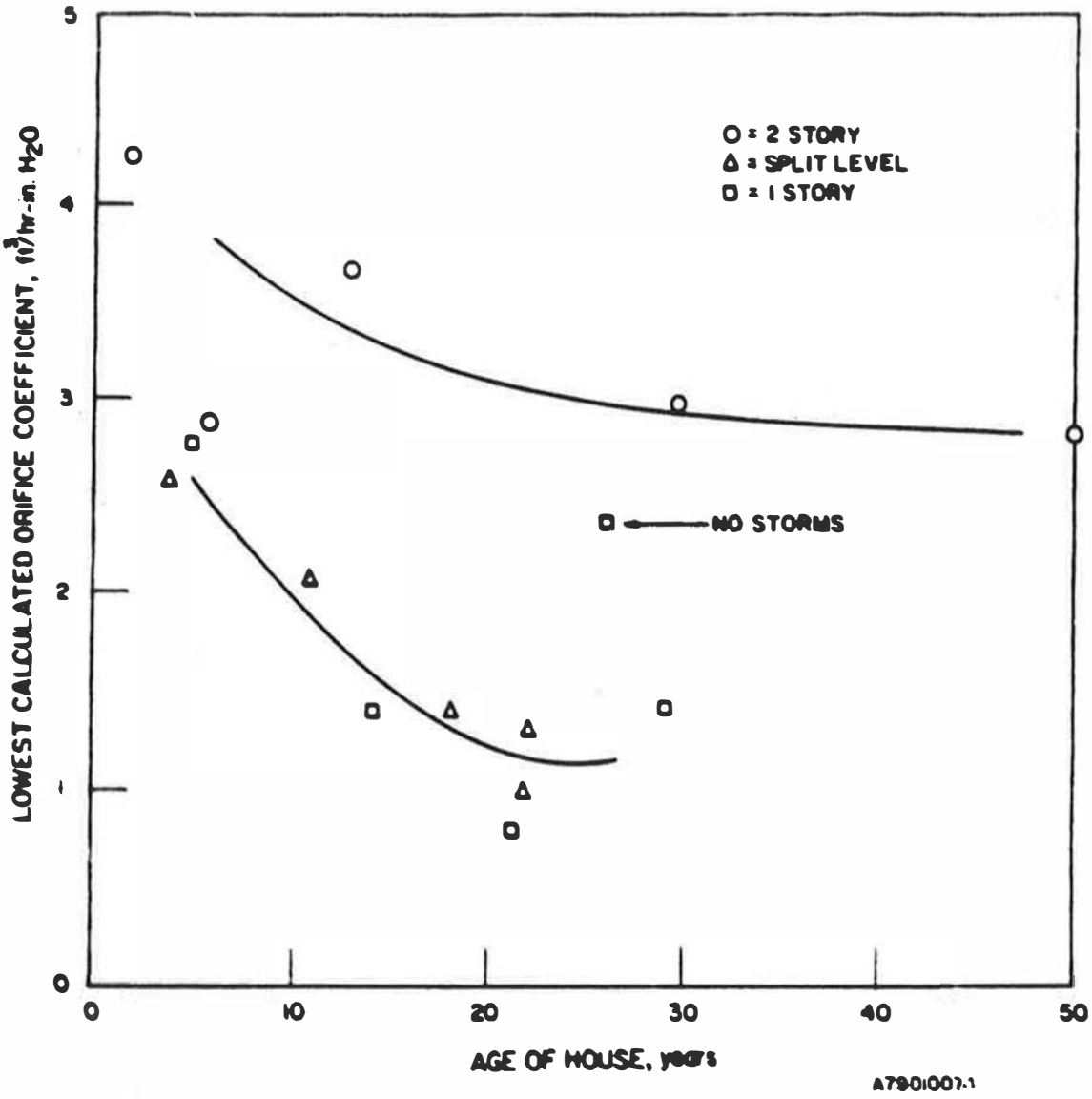

Figure 39. APPARENT EFFECT OF AGE ON CALCULATED ORIFICE COEFFICIENT

2. Comparisons With Data From the Ranch Home

The basic air infiltration models (with chimney blocked) have also been evaluated against the data from the ranch home, for which we have more complete data on leakage characteristics. The results of the comparison are shown in Table 8. For this case, orifice coefficients were calculated assuming the following three different levels of crack lengths:

- Door and window perimeter cracks only
- Door and window perimeter and framing cracks
- Door and window perimeter plus framing cracks plus sill plate cracks.

It should be noted in Table 8 that the average calculated orifice coefficient for 20 discrete data points decreases steadily from 5.2, when only the door and window cracks are considered, to 2.8, when framing cracks are included, to 1.7, when sill plate cracks are also included. The latter coefficient is well within the range that we would predict since the house is considered to be a "tight" house.

Also of considerable interest is the consistency of the calculated orifice coefficients under different ambient conditions. It should be noted that for case 3, in which all sill plate leakage is included, all calculated orifice coefficients, with the exception of two, are within the narrow range from 0.7 to 2.1. The two exceptions are for measurements A and C made under practically no driving force conditions, under which infiltration is dominated by the blower action. It should also be noted that for data obtained in the wind dominated regime (runs B, F, O, and T), the coefficients are lowest (0.7 to 1.2) with an average of 1.0. These values are considered closer to the real values since the blower contribution is minimized.

The results of Table 8 also show that the calculated orifice coefficients correlated fairly well with wind speed and direction, as shown in Figure 40. It should be noted that the coefficients tend to decrease with increasing wind speed, and that the lowest coefficients are those in which the wind direction is other than south. This is probably associated with the fact that the south wall is blank (no windows or doors). This suggests that the higher orifice coefficients required, when the wind is from the south, are due to the negative pressure induced on the north side for which the model does not account.

Table 8. CALCULATED ORIFICE COEFFICIENTS FOR THE RANCH TEST HOME

Run	Wind Speed, mph	Wind Direction	T_o °F	Regime	Infiltration Rate CFM	Orifice Coefficient CFM/ft/in$_{H_2O}$ Case* 1	Case* 2	Case* 3
A	0	-	66	Buoyancy	27	10.5	6.2	4.4
B	5	SE	78	Wind	27	3.6	1.8	1.2
C	2	S	67	Mixed	14	6.6	3.1	2.0
D	2	SW	74	Mixed	17	6.8	3.1	2.1
E	2	S	60	Mixed		4.0	1.9	1.3
F	5	SE	57	Wind	24	10.5	10.5	1.2
G	3	S	46	Mixed	19	4.5	2.1	3.7
H	3	N	58	Mixed	17	3.5	1.6	1.2
I	8	S	60	Mixed	17	7.2	3.4	1.6
J	6	W	40	Mixed	22	2,7	1.3	0.9
K	2	S	33	Buoyancy	27	4.3	2.0	1.5
L	4	S	30	Mixed	29	5.1	2.4	1.6
M	10	S	40	Mixed	27	5.9	2.8	1.5
N	6	S	40	Mixed	33	6.3	2.9	1.9
O	11	W	34	Wind	28	2.1	1.0	0.7
P	5	S	33	Mixed	19	4.4	1.6	1.1
Q	7	S	42	Mixed	14	4.1	1.9	1.2
R	4	SE	8	Buoyancy	41	5.3	2.5	1.8
S	3	S	5	Buoyancy	41	5.7	2.7	1.9
T	8	N	30	Wind	32	2.4	1.1	0.9

Case 1 Window and door perimeters only
2 Window and door perimeters and framing
3 Window and door perimeters, framing, plus sill plate

A79040838

Figure 40. VARIATION OF CALCULATED ORIFICE COEFFICIENT WITH WIND SPEED AND DIRECTION (Ranch Type Home)

In summary, these results are significant and show that:

- The average orifice coefficient of 0.7 to 1.0 indicated is well within the range expected for a tight house. They indicate that the bulk of the leakage, at least for ranch type structures, can be explained in terms of door and window parameters plus framing and sill plate crackage.
- The effect of blower induced infiltration is observable.
- The effect of wind direction (particulary south vs. north or west) suggests that the aerodynamically induced negative pressures on the leeward sides of the house may be important. This is not unexpected.

B. Comparison With Data From Homes With Chimneys

The basic infiltration model was modified to include the effect of the presence and operation of the gas furnace/vent system. This involved the introduction of the previously[9] developed flue flow sub-model into the program so that the overall model calculates both chimney flow and total infiltration, at most balances. The input data for the flue flow sub-model include furnace input rating, flue temperature, and vent system dimensions.

As in the previous case, the model was used to calculate the equivalent orifice coefficients required to make the calculated infiltration rates equal to the measured infiltration rates, under two different conditions:

- With the chimney flow calculated by the flue flow sub-model at mass balance
- With the flue flow model bypassed and the measured chimney flows substituted.

In this manner, the model can be evaluated in terms of the effect of the measured chimney flow on infiltration (i.e. magnitude of orifice coefficients, with chimney open, compared with those required when flue is blocked) in terms of the effect of the overall infiltration dynamics on flue flow (i.e., by comparison of calculated versus measured chimney flows).

For a given set of measurements under the same ambient conditions, the orifice coefficients required for equivalence should be the same with the flue blocked and with the flue open and the furnace on. Such a comparison is shown in Figure 41. The data indicate that the orifice coefficients calculated for the flue open and the flue closed cases agree reasonably well

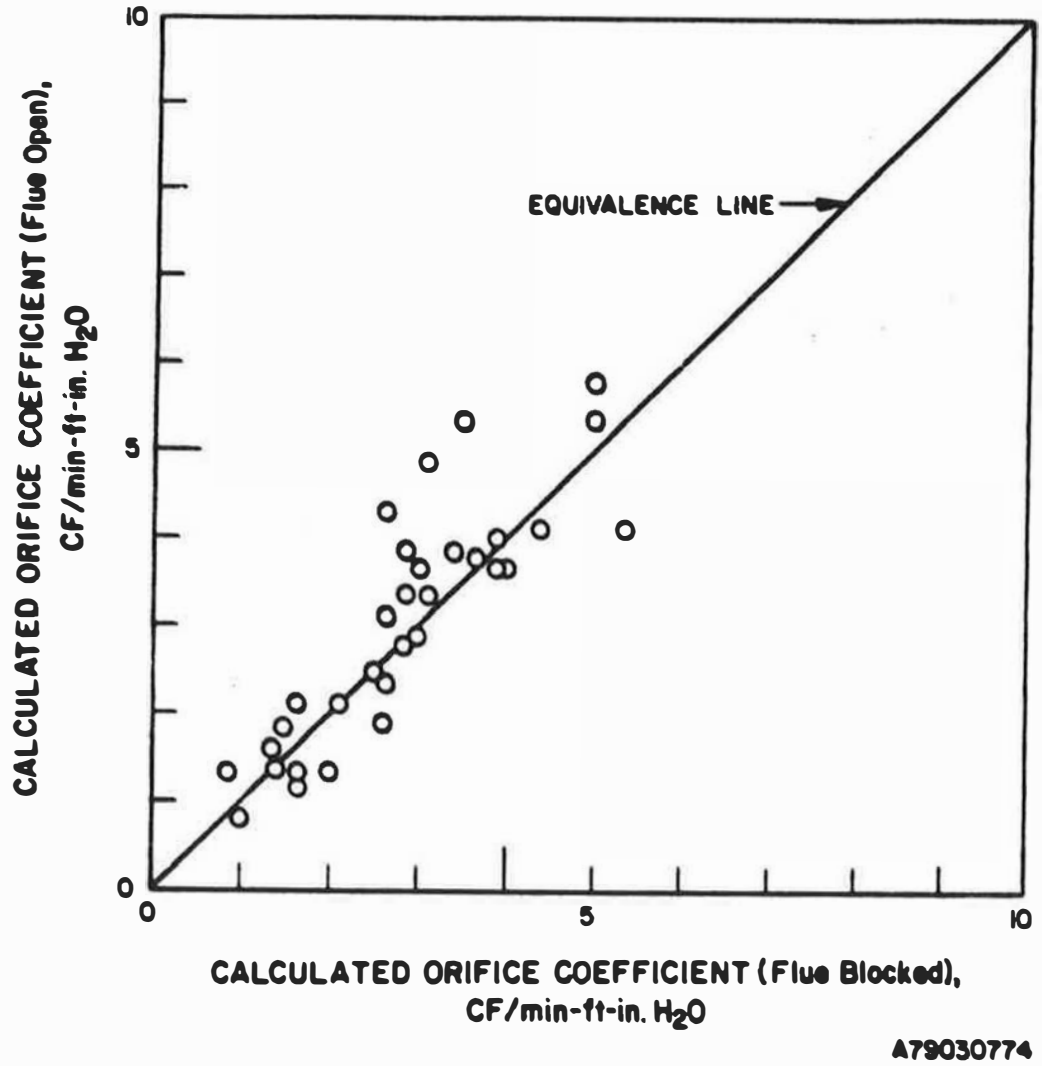

Figure 41. CORRESPONDENCE BETWEEN CALCULATED ORIFICE COEFFICIENTS FOR FLUE-CLOSED AND FLUE-OPEN AND FURNACE OPERATING

with each other, with a standard deviation of 0.4 unit.

Figure 41 also shows that data from four homes (Nos. 6, 2, 7, and 5) show a greater scatter than the above standard deviation of up to 1.9 units of the orifice coefficient. This disagreement in calculated orifice coefficient does not appear to be associated with K_x/K_i ratio, control regime, or the agreement between calculated and measured chimney flows. It does, however, appear to be associated with high ϕ values. In three of the five cases, the ϕ value was greater than 1.0 and, in the other two cases, greater than 0.7. These disagreements suggest that the air infiltration data in the 5 instances may be in error. The available infiltration data from these homes have not yet been of sufficient quantity to conduct a comparison between measured chimney flows with those calculated with the combined infiltration/ chimney flow model.

REFERENCES CITED

1. Alereza, T., "Report on Progress Review Workshop," Geomet, ASHRAE Special Project #17, September 28, 1977.

2. American Society of Heating, Refrigerating, and Air-Conditioning Engineers, Inc., Handbook of Fundamentals. New York, 1972.

3. Bahnfleth, D.R., et al., "Measurement of Infiltration in Two Residences, Part I," ASHRAE Trans. 63, 439-452 (1957).

4. Coblentz, C.W. and Achenbach, P.R., "Field Measurements of Air Infiltration in Ten Electrically Heated Houses," ASHRAE Trans. 69, 358-65 (1963).

5. Dick, J.B., "Experimental Studies in Natural Ventilation of Houses," IHVE J. 17, 420-466 (1964) December.

6. Gibson, U.E. and Cawley, R.E., "The Heat Pump Solar Collector Interface — A Practical Experiment," Appliance Eng. 68-77 (1977) August.

7. Harrje, D.T., "Variations in Infiltration in Townhouses Before and After Retrofit." Paper presented at the E-6 Symposium on Air Infiltration and Air Change Rate Measurement, ASTM March Committee Week, Washington, D.C., March 13, 1978.

8. Hittman Associates, Inc., "Residential Energy Consumption in Single-Family Housing, "Report No. HUD-HAI-2. Columbia, MD., March 1973.

9. Institute of Gas Technology, Experimental Characteristics of the Gas Furnace-Water Heater-Chimney-Home System," A.G.A. Project HC-4-33. Chicago, March 1977.

10. Institute of Gas Technology, "Experimental Testing of an Automatic Flue Damper System," A.G.A. Project HA-4-31. Chicago, November 1975.

11. Janssen, J.E., Torborg, R.H. and Bonne, U., "Measurement of Heating System Dynamics for Computation of Seasonal Efficiency," ASHRAE Trans. 83, Part 2, Paper No. 2460, 1977.

12. Jorden, R.C. et al., "Infiltration Measurements in Two Research Houses," ASHRAE Trans. 69, 344-350 (1963).

13. Laschober, R.R. and Healy, J.H., "Statistical Analysis of Air Leakage in Split Level Residences," ASHRAE Trans. 70, 364-374 (1964).

14. Malik, N., "Field Studies of Dependence of Air Infiltration on Outside Temperature and Wind," Energy & Bldgs. 1, 281-292 (1977/78).

REFERENCES CITED, Cont.

15. Sandu. D.M., FORTRAN IV Program to Calculate Air Infiltration in Buildings, National Research Council of Canada, Research Computer Program, No. 37, May 1974.

16. Shaw, C.Y. and Tamura, G.T., "The Calculation of Air Infiltration Rates Caused by Wind and Stack Action for Tall Buildings," ASHRAE Trans. 83, Part 2, Paper No. 2459, 1977.

17. Sinden, F.W., "Wind Temperature and Natural Ventilation – Theoretical Considerations," Energy & Bldgs. 1, 275-280 (1977/78).

18. Tamura, G.T., "Measurement of Air Leakage Characteristics of House Enclosures," Paper No. 2339 presented at ASHRAE Meeting, Atlantic City, New Jersey, January 1975.

19. Tamura, G.T. and Wilson, A.G., "Air Leakage – Pressure Measurements on Two Occupied Houses," ASHRAE Trans. 70, 110-119 (1964).

20. Institute of Gas Technology, "Field Verification of the Gas-Furnace-Water Heater-Chimney-Home Flue Loss Model," Final Rep. Am. Gas Assoc. HC-4-33, January 1978.

21. Macriss, R.A. et al., "Energy Efficiency for Appliances, Home Heating Equipment, Furnaces and Humidifiers," Final Report, U.S. - FEA Subcontract No. CR-04-60725-00-001 November 1977.